Enhancing the absorption properties of acoustic porous plates by periodically embedding Helmholtz resonators

J.-P. Groby,[a] C. Lagarrigue, B. Brouard, O. Dazel, and V. Tournat
Laboratoire d'Acoustique de l'Université du Maine, L'Université Nantes Angers Le Mans, Université du Maine, CNRS, UMR-6613 CNRS, Avenue Olivier Messiaen, 72085 Le Mans, France

B. Nennig
Laboratoire d'Ingénierie des Systèmes Mécaniques et des Matériaux, EA 2336, Supméca, 3 Rue Fernand Hainaut, 93407 Saint-Ouen Cedex, France

(Received 14 February 2014; revised 3 October 2014; accepted 19 November 2014)

This paper studies the acoustical properties of hard-backed porous layers with periodically embedded air filled Helmholtz resonators. It is demonstrated that some enhancements in the acoustic absorption coefficient can be achieved in the viscous and inertial regimes at wavelengths much larger than the layer thickness. This enhancement is attributed to the excitation of two specific modes: Helmholtz resonance in the viscous regime and a trapped mode in the inertial regime. The enhancement in the absorption that is attributed to the Helmholtz resonance can be further improved when a small amount of porous material is removed from the resonator necks. In this way the frequency range in which these porous materials exhibit high values of the absorption coefficient can be extended by using Helmholtz resonators with a range of carefully tuned neck lengths.
 [http://dx.doi.org/10.1121/1.4904534]

[KVH] Pages: 273–280

I. INTRODUCTION

Air saturated porous materials, namely, foams and wools, are often used as sound absorbing materials. Nevertheless, they suffer from a lack of absorption efficiency at low frequencies which is inherent to their absorption mechanisms, even when used as optimized multilayer or graded porous materials. Actually, these mechanisms only rely on viscous and thermal losses. In the inertial and adiabatic regimes,[1] when the frequencies are higher than the Biot frequency f_ν, relatively thin porous plates provide excellent tools to absorb sound, but they fail in the viscous and isothermal regimes, i.e., at lower frequencies. In the inertial and adiabatic regimes, the acoustic pressure satisfies an Helmholtz equation, with losses, while in the viscous and isothermal regimes, it satisfies a diffusion equation.

These last decades, several solutions have been proposed to overcome this lack of efficiency. They usually consist in coupling the viscous and thermal losses of porous materials with additional absorption mechanisms, mainly associated with resonance phenomenon arising from the addition of heterogeneities.

(1) The absorption enhancement of double porosity materials[2–4] arises from resonances of the microporous material (pressure diffusion mechanisms) excited by the macropores in case of a initial porous material layer. The theory describing the behavior of these materials is well established by homogenization. For high contrast flow resistivity between the micro and the macro porous materials, the absorption enhancement is obtained at the diffusion frequency f_d, which only depends on the geometry and organization of the holes in infinite double porosity medium. For an optimal absorption efficiency of a double porosity plate, f_d should be in practice around the frequency for which the penetration depth is of the same order of the homogeneous microporous plate thickness. This theory can also be used to model porogranular materials,[5] but the low frequency properties of activated carbon (large resistivity contrast) cannot be completely explained by their double porosity structure, but also by sorption mechanisms.

(2) Another possibility consists in plugging dead-end pores, i.e., quarter-wavelength resonators, on open pores to create dead-end porosity materials.[6] This results in anomalies in the absorption coefficient when the wavelength is on the order of the dead-end pore length. Nevertheless, the absorption enhancement is still not completely understood and is subjected to the inertial regime with regards to the dead-end pores. Moreover, the current manufacturing process involving salt grains and liquid metal does not yet offer the possibility of the full control over the densities and the lengths of the dead-end pores.

(3) Metaporous materials, in which modes are excited, trapping the energy between periodic rigid inclusions embedded in the porous plate and the rigid backing or in the inclusions themselves (split-ring resonators), have been proposed. The absorption properties of the porous plate are enhanced at lower frequencies than the quarter wavelength frequency,[7,8] when the absorption of the initial plate is not unity at this frequency. When split-ring resonators are correctly arranged and coupled with the rigid backing, the absorption coefficient can be higher than 0.9 for wavelengths smaller than 10 times the material thickness and over a large frequency band, which largely

[a]Author to whom correspondence should be addressed. Electronic mail: jean-philippe.groby@univ-lemans.fr

overcome the usual limit of the quarter wavelength.[9] Moreover, this last technique is only efficient in the inertial regime, because the split-ring resonators are filled by porous materials enabling to lower their resonance frequency. This means that it is possible to absorb the energy at frequencies higher than the Biot frequency f_ν with very thin structures, but that an increase of the metaporous plate thickness does not necessarily lead to enhanced absorption for lower frequencies. Indeed, the resonators cannot resonate when filled by a porous material in the viscous and isothermal regime, because the pressure field satisfies a diffusion equation. Adding periodic air cavities to the rigid backing enable to partially solve this problem, but it requires either deep cavity or large lateral periodicity.[10,11]

Recently, membrane-type metamaterials that exhibit nearly total reflection at an anti-resonance frequency[12] or nearly total absorption due to the flapping motion of asymmetric rigid platelets added to the membrane[13] have been proposed, but their absorption properties are limited in the metamaterial resonance frequency range. The use of Helmholtz resonators as sound attenuators in ducts has already been proposed,[14–16] but not their use together with acoustic porous materials as common sound absorbing materials. Metamaterials have induced a revival of interest in Helmholtz resonators (HRs) to manufacture negative bulk modulus and mass density materials.[17,18] In Ref. 17, split hollow sphere were embedded in a sponge matrix. This material exhibit negative bulk modulus at the HR resonance. The effective properties, mainly wave velocity and effective stiffness, of an infinite porous material with embedded resonators were recently investigated in Ref. 19 by homogenization. The scale separation assumption implies long wavelength condition. Different behavior depending on the ratio between the HR resonant frequency f_r and f_ν were exhibited, while negative stiffness was demonstrated around the resonance frequency, but the absorption properties of the structure were not analyzed.

The aim of this paper is to improve the absorbing properties of a porous material by periodically embedding HRs. The analysis is performed in the viscous and inertial regimes of the porous material thanks to a finite element method.[20] HR has two main effects: (1) an additional internal resonance, that dominates the absorbing material response at f_r; (2) another additional resonance, that dominates the absorbing properties at higher frequencies.[20] Both effects will be investigated in order to enhanced absorption on a wide frequency range without long-wavelength limitation. The paper is organized as follows: The configurations and the main assumptions are described and a parametric study is then presented; Finally, experimental validations are proposed. These last results illustrate the main trends of the parametric study on practical cases.

II. PRELIMINARY REMARKS

The absorption enhancement of metaporous materials both in viscous and inertial regimes is a multi and interconnected parameter optimization process, which depends on the porous material parameters, material thickness, dimensions of the inclusions, dimensions of the resonators, and periodicities. Here, we will focus on the influence of the periodic embedment of HRs around their resonance, keeping in mind previous conclusions on metaporous materials (Refs. 7–9 and 20):

(1) If the absorption is not total at the quarter-wavelength resonance, the embedment of periodic inclusions in a porous slab attached to a rigid backing leads to an increase of this absorption peak and shifts this peak to lower frequency. This mainly depends on the volume of the inclusion at low frequency. A total absorption peak can be obtained if the required filling fraction can be reached. This filling fraction depend on the parameters of the porous materials. Still increasing the filling fraction after total absorption has been reached, deteriorates the absorption coefficient, while still shifting the maximum absorption peak to lower frequencies.
(2) If the absorption coefficient is already total at the quarter-wavelength resonance, embedding periodic inclusions shift this peak to low frequency, but the absorption is deteriorated.
(3) The shift to low frequency depends on the filling fraction and on the position of the inclusion barycenter. The larger is the distance between the inclusion and the rigid backing, the lower is the absorption peak frequency. This absorption enhancement is subjected to the periodic set of inclusions and its interaction with its image, to material parameters, but not directly to the plate thickness.[7,20]
(4) When the total absorption peak is obtained, the acoustic energy is trapped between the inclusion and the rigid backing.
(5) When a total absorption peak can be obtained, the required filling fraction is larger in 3D than in 2D.[20] Moreover, the frequency at which this total absorption peaks is reached is higher in 3D than in 2D for a given material properties and thickness.

The studied configurations also derived from two-dimensional ones, because it enables lower filling fraction and larger resonator volume. The neck of the embedded HRs will not be outer but rather inner also enabling larger resonator volume and larger filling fraction, both being constrain by the structure thickness. Inner neck enable to save volume when compared to outer neck. The studied HRs derive from the configuration studied in Ref. 21, without outer neck. Moreover, the HRs being embedded in a porous material the viscous dissipation in the neck is neglected when compared to the dissipation in the porous material.

III. FORMULATION OF THE PROBLEM

A. Description of the configuration

A parallelepiped unit cell of the 3D scattering problem together with a sketch of one HR are shown in Fig. 1. Before the addition of the HR, the layer is a rigid frame porous material saturated by air (e.g., a foam or a wool) which is modeled as a macroscopically homogeneous equivalent fluid M^p using the Johnson-Champoux-Allard model.[1,22] The upper

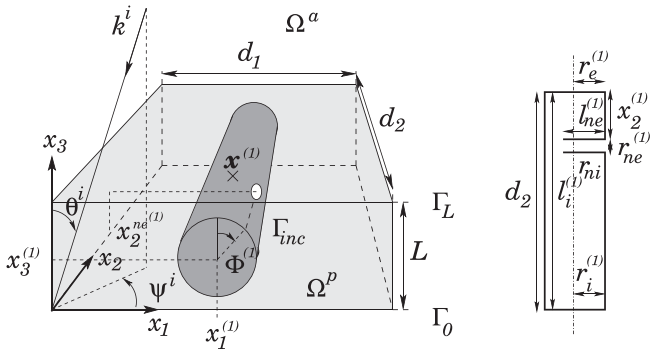

FIG. 1. Example of a **d**-periodic fluid-like porous sheet backed by a rigid wall with a periodic inclusion embedded in.

and lower flat and mutually parallel boundaries of the layer, whose x_3 coordinates are L and 0, are designated by Γ_L and Γ_0, respectively. The upper semi-infinite material M^a, i.e., the ambient fluid that occupies Ω^a, and M^p are in a firm contact at the boundary Γ_L, i.e., the pressure and normal velocity are continuous across Γ_L. A Neumann type boundary condition is applied on Γ_0, i.e., the normal velocity vanishes on Γ_0.

HRs deriving from 2D configuration are embedded in the porous layer with a spatial periodicity $\mathbf{d} = \langle d_1, d_2, 0\rangle$ and create a two-dimensional diffraction grating in the plane x_1–x_2. The lengths of the HRs are d_2, while the lengths of the HR cavities are $l_i^{(j)}$, outer and inner radii are $r_e^{(j)}$ and $r_i^{(j)}$. HRs positions are referred to as the barycenter of the outer volume $(x_1^{(j)}, d_2/2, x_3^{(j)})$. HR necks are cylinders of circular cross-sections of lengths $l_n^{(j)}$. The outer and inner radii of the neck are $r_{ne}^{(j)}$ and $r_{ni}^{(j)}$, respectively. The neck x_2-coordinates are $x_{2n}^{(j)}$, while their angular positions are $\Phi^{(j)}$. The inner volume and the neck of the HRs are filled with air medium.

The incident wave propagates in Ω^a and is expressed by $p^i(\mathbf{x}) = A^i e^{\mathrm{i}(k_1^i x_1 + k_2^i x_2 - k_3^{ai}(x_3 - L))}$, wherein $k_1^i = -k^a \sin\theta^i \cos\psi^i$, $k_2^i = -k^a \sin\theta^i \sin\psi^i$, $k_3^{ai} = k^a \cos\theta^i$, and $A^i = A^i(\omega)$ is the signal spectrum. The azimuth of the incident wave vector is ψ^i and its elevation θ^i.

In each domain Ω^α ($\alpha = a,p$), the pressure field fulfills the Helmholtz equation

$$\nabla \cdot \left(\frac{1}{\rho^\alpha}\nabla p^\alpha\right) + \frac{(k^\alpha)^2}{\rho^\alpha} p^\alpha = 0, \tag{1}$$

with the density ρ^α and the wave number $k^\alpha = \omega/c^\alpha$, defined as the ratio between the angular frequency ω and the sound speed c^α.

As the problem is periodic and the excitation is due to a plane wave, each field (X) satisfies the Floquet-Bloch relation

$$X(\mathbf{x} + \mathbf{d}) = X(\mathbf{x}) e^{\mathrm{i}\mathbf{k}_\perp^i \cdot \mathbf{d}}, \tag{2}$$

where $\mathbf{k}_\perp^i = \langle k_1^i, k_2^i, 0\rangle$ is the in-plane component of the incident wave number. Consequently, it suffices to examine the field in the elementary cell of the material to get the fields, via the Floquet relation, in the other cells. The periodic wave equation is solved with a FE method. This FE method as well as the absorption coefficient calculation method are described and validated in Ref. 20.

B. Material modeling

The rigid frame porous material is modeled using the Johnson-Champoux-Allard model. The compressibility and density, linked to the sound speed through $c^p = \sqrt{1/(K^p \rho^p)}$ are[1,22]

$$\frac{1}{K^p} = \frac{\gamma P_0}{\phi\left(\gamma - (\gamma-1)\left[1 + \mathrm{i}\left(\frac{\omega_c'}{\mathrm{Pr}\,\omega}\right) G(\mathrm{Pr}\,\omega)\right]^{-1}\right)},$$
$$\rho^p = \frac{\rho^a \alpha_\infty}{\phi}\left(1 + \mathrm{i}\,\frac{\omega_\nu}{\omega} F(\omega)\right), \tag{3}$$

wherein $\omega_\nu = 2\pi f_\nu = \sigma\phi/\rho^a\alpha_\infty$ is the angular Biot frequency, $\omega_c' = \sigma'\phi/\rho^a\alpha_\infty$ is the adiabatic/isothermal crossover angular frequency, γ the specific heat ratio, P_0 the atmospheric pressure, Pr the Prandtl number, ρ^a the density of the fluid in the (interconnected) pores, ϕ the porosity, α_∞ the tortuosity, σ the flow resistivity, and σ' the thermal resistivity. The correction functions $G(\mathrm{Pr}\,\omega)$ (Ref. 1) and $F(\omega)$ (Ref. 22) are given by

$$G(\mathrm{Pr}\,\omega) = \sqrt{1 - \mathrm{i}\eta\rho^a \mathrm{Pr}\,\omega\left(\frac{2\alpha_\infty}{\sigma'\phi\Lambda'}\right)^2},$$
$$F(\omega) = \sqrt{1 - \mathrm{i}\eta\rho^a\omega\left(\frac{2\alpha_\infty}{\sigma\phi\Lambda}\right)^2}, \tag{4}$$

where η is the viscosity of the fluid, Λ' the thermal characteristic length, and Λ the viscous characteristic length. The thermal resistivity is related to the thermal characteristic length[1] through $\sigma' = 8\alpha_\infty\eta/\phi\Lambda'^2$.

IV. PARAMETRIC STUDY, RESULTS, AND DISCUSSION

In this section, the influence of the main parameters will be investigated for one HR per period and two HRs per period. First, the influence of the ratio f_r/f_ν, which summarizes the porous material main characteristics, is studied. Then, trends for the main geometric quantities, i.e., the neck orientation and the filling fraction, are drawn. Finally, the influence of the angle of the incident plane wave is examined to evaluate the absorption of this material for practical applications submitted to incident diffuse field.

In all simulations and experimental validations, the thickness of the porous slab, periodicity along the x_2 direction, x_3 position of the HRs, and inner length of the HRs as well as the outer and inner radius of the neck are fixed at $L = 22.5$ mm, $d_2 = 42$ mm, $l_i^{(j)} = 40$ mm, $x_3^{(j)} = 11.5$ mm, $r_{ne}^{(j)} = 2$ mm, and $r_{ne}^{(j)} = 1.5$ mm. The inclusion are not placed at $x_3^{(j)} = L/2$, but at a larger x_3-coordinates, enabling a lower frequency of the trap mode. The volume of the HRs can be modified by changing the outer and inner radius (and the neck length), while the neck characteristics can be modified through their lengths and orientations. The dimensions of the different studied configuration are reported in Table I.

TABLE I. Dimensions of the main studied configurations.

Configuration	d_1 (mm)	$x_1^{(j)}$ (mm)	$x_{2n}^{(j)}$ (mm)	$(r_e^{(j)}, r_i^{(j)})$	$\Phi^{(j)}$	$l_{ne}^{(j)}$ (mm)
$C1$	21	10.5	12	(8,6.8)	0	10
$C2$	21	10.5	12	(8,6.8)	$0, \pi/2, \pi$	10
$C3$	21, 26, 31, 36	10.5, 13, 15.5, 18	12	(8,6.8)	0	10
$C4$	42	10.5	12	(8,6.8)	0	11
		31.5	12	(8,6.8)	0	10, 8, 6, 4
$C5$	42	10.5	12	(8,6.8)	0	11
		31.5	12	(8,6.8), (7,6.8), (6,6.8)	0	10, 9, 8
$C6$	42	11.5	12	(8,6.8)	0	10
		30.5	12	(8,6.8)	0	10
$C7$	42	11.5	12	(8,6.8)	0	11
		30.5	12	(8,6.8)	0	7

Three different materials are considered: A small flow resistivity foam $S1$ (refereed to as blue foam in Ref. 23), a medium flow resistivity Melamine foam $S2$, and a wool $S3$ (GR 32 nu, ISOVER). These materials have been chosen in such a way that the ratio of resonant frequency of the HR over their Biot frequencies are $f_r/f_\nu \ll 1$ for $S3$, $f_r/f_\nu \leq 1$ for $S2$, and $f_r/f_\nu \geq 1$ for $S1$, respectively. The parameters of these three porous materials are reported in Table II and have been evaluated using the traditional methods (Flowmeter for the resistivity and ultrasonic methods for the 4 other parameters, together with a cross-validation by impedance tube measurement) described in Ref. 24.

A. Results for one HR per period

HRs are designed with $l_n = 10\,\text{mm}$ leading to configuration $C1$. The HRs resonate, in first approximation, at $f_r = (c^a/2\pi)\sqrt{A/Vl_{eff}} = 540\,\text{Hz}$, where $A = \pi r_{ni}^2$ is the cross-section area of the neck, $V = l_i \pi r_i^2 - (l_n - r_{ne} + r_{ni})\pi r_{ne}^2$ the volume of the resonators, and $l_{eff} = l_n + 8r_{ne}/3\pi$ is the effective length of the neck.[25] This frequency is approximated because no exact formula exists for inner neck resonators. The main advantage of using HRs is that they can resonate at a very low frequency for small dimensions[19] compared to other 2D shape resonators (double or simple split-ring resonators).

1. Influence of the ratio f_r/f_ν and absorption at f_r

The effect of the ratio f_r/f_ν is first investigated. Figures 2(a), 2(b), and 2(c) depict the absorption coefficients of configuration $C1$, when the porous material is $S1$, $S2$, and $S3$, respectively. The resonance of the HR leads to absorption enhancement at f_r whatever the porous material properties in particular, the flow resistivity, i.e., whatever the Biot frequency. Nevertheless, this enhancement is large when f_r/f_ν is larger than or close to unity and decreases when f_r becomes smaller than f_ν [see Fig. 2(d)]. This conclusion can be expected from those driven from the analysis of the effective parameters of infinite porous materials with weak concentration of HRs.[16] However, in the present article, the HR density is large so that the considered configurations do not fit homogenization requirements. When f_r/f_ν is larger than unity, the HRs resonance already leads to a quasi-total absorption peak. The associated wavelength in the air is 27 times larger than the sample thickness at f_r. This means that the absorption properties of porous materials in the inertial regime can be enhanced by embedding air filled HRs, but also that this type of structure can accurately absorb sound for wavelengths much larger than the sample thickness. For lower ratio f_r/f_ν, modifying the input impedance of the HRs by removing small amount of porous material just in front of the neck leads to a larger absorption peak of the configuration at f_r [see Fig. 2(d)]. This is due to a lowering of the input impedance, which enables a larger energy advection. Therefore, a larger velocity gradient in the neck and in its vicinity is induced leading to a larger viscous dissipation. Nevertheless, this is associated with a narrowing of the absorption peak.

TABLE II. Acoustical parameters of the porous material constituting the sheet of thickness L.

	ϕ	α_∞	Λ (μm)	Λ' (μm)	σ (N s m^{-4})
$S1$	0.96	1.07	273	672	2843
$S2$	0.98	1.02	180	240	12000
$S3$	0.97	1.03	56	85	28500

At higher frequency, the excitation of the trapped mode leads to a wide enhanced absorption peak at lower frequency than the quarter wavelength resonance one when $S1$ and $S2$ material are used, while the absorption is lower in case of $S3$ material. Indeed, the absorption of $S3$ material is nearly optimal and the addition of a periodic set of rigid inclusions degrades its performances [see point (1) of Sec. II]. An absorption enhancement would have been possible in this last case if the layer thickness would have been smaller. An important remark is that the outer radius has not been optimized neither for $S1$ nor $S2$, therefore the absorption is not unity at the trapped mode frequency. In particular, the required filling fraction is around $ff = V_{\text{HR}}/V_{\text{cell}} = 0.4255$ for $S2$ for a total absorption peak and is larger in the present case. The first resonance of the HR is excited in each cases around 4100 Hz, while the absorption is lower at the Bragg interference around 6500 Hz. Note that the mode of the backed layer possibly excited by the periodicity d_2 is not excited. This means that the configuration behavior is close to the one of a two-dimensional configuration, i.e., the neck has a weak influence on the results at high frequency.

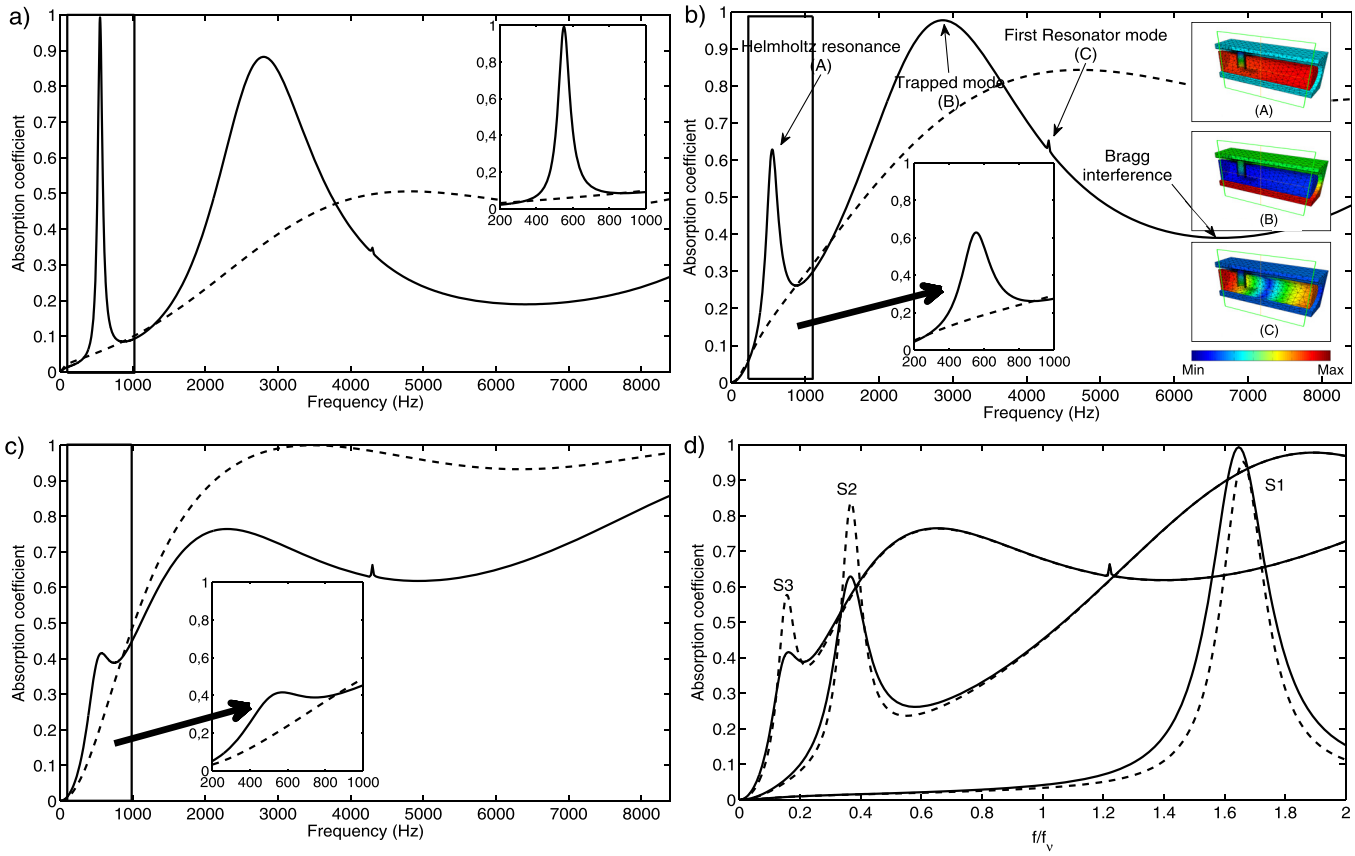

FIG. 2. (Color online) Absorption coefficient of configuration $C1$ (black curves) and associated homogeneous sheet (dashed curves) occupied by the foam (a) $S1, f_r/f_\nu \geq 1$, (b) $S2, f_r/f_\nu \leq 1$, and (c) $S3, f_r/f_\nu \ll 1$, when excited at normal incidence. The insets show zooms of the absorption coefficient around the HRs frequencies, and the snapshot of the sound pressure field at the frequency of the HR resonance, of the trapped mode, and of the first HR resonance. (d) absorption coefficient of configuration $C1$ occupied by the foam $S1$, $S2$ and $S3$ in function of f/f_ν (solid line) and with a small amount of porous material removed in front the neck (dashed line).

2. Influence of the neck orientation and filling fraction

Both the influence of neck orientation and of the filling fraction are then investigated for configuration $C1$ and $S2$ porous material in Figs. 3(a) and 3(b), respectively. The largest absorption enhancement is obtained when the neck is facing the air interface, i.e., $\Phi = 0$. In this configuration, the energy advection by the HR is large. When the neck is facing the rigid backing, i.e., $\Phi = \pi$, the HR and the rigid backing are coupled, which lowers f_r, but the value of the absorption peak is then lower because of a poor energy advection. The presence of both the surrounding inclusion and the rigid backing can be interpreted as a neck extension that lowers f_r when the neck face the rigid backing. The lowering of the absorption amplitude can be interpreted in terms of penetration depth: the energy trapped in the HR is larger when the

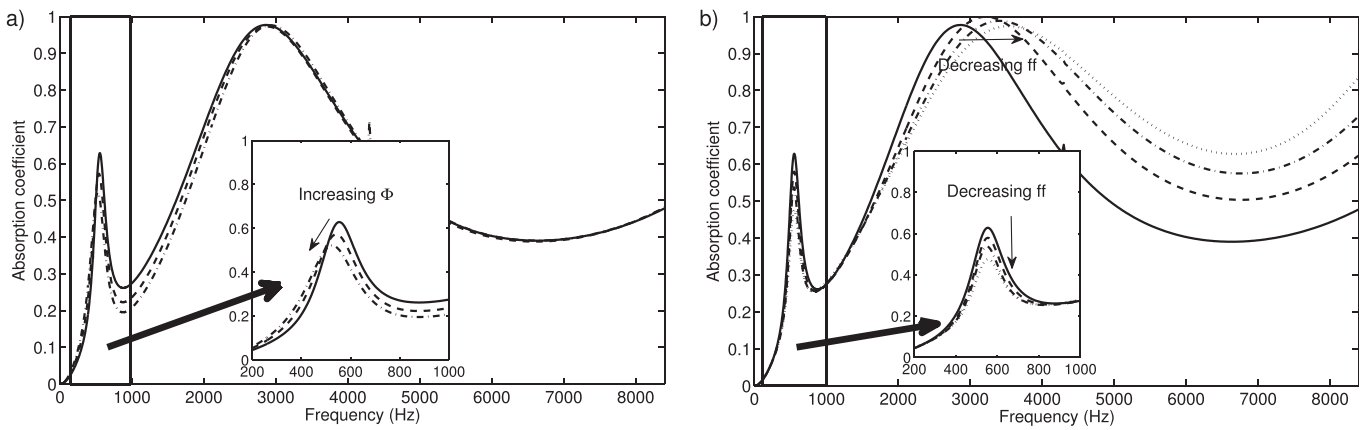

FIG. 3. Absorption coefficient of (a) configurations $C2$: $\Phi = 0$ solid curve, $\Phi = \pi/2$ dashed curve and $\Phi = \pi$ dashed-dotted curve; and (b) configuration $C3$: $d_1 = 21$ mm solid curve, $d_1 = 26$ mm dashed curve, $d_1 = 31$ mm dashed-dotted curve and $d_1 = 36$ mm dotted curve. The material layer is the foam $S2$ and the configuration is excited at normal incidence. The insets show zooms of the absorption coefficient around the HRs frequencies.

neck is close to the interface than when the neck is deep because it penetrates more easily. Increasing Φ, lower the absorption peak associated with the resonance frequency, similarly to what was found in case of split-ring resonators,[9] but lower the amplitude of the absorption peak. The absorption peak associated with the excitation of the trapped mode is weakly affected by a modification of Φ. Decreasing *ff* by increasing the periodicity d_1 lowers the amplitude of the absorption peak associated with the HRs resonance, while largely affects both position and amplitude of trapped mode associated peak. In particular, the optimal filling fraction being around $ff = 0.4255$, the absorption peak is close to unity when $d_1 = 26$ mm.

The absorption efficiency related to the HR resonance is largely affected by their concentration.

3. Influence of the angle of incidence

The influence of the angle of incidence is finally investigated for configuration $C1$ and $S2$ porous material in Fig. 4 for various elevation at fixed azimuth $\psi^i = 0$. While a modification of θ^i largely modifies the absorption curve, a variation of ψ^i at fixed θ^i does not strongly affect the absorption curves below 6000 Hz. Nevertheless, the absorption curves have been found symmetric for ψ^i varying from $[0; \pi/2]$ and $[\pi/2; \pi]$, whose fact again is an argument for a two-dimensional like configuration. The frequency of the absorption peaks association the HRs excitation is by definition not affected by the variation of θ^i, while the one associated with the trapped mode is. This is due to the real and localized resonant features of the HR which is not affected by the excitation. Increasing θ^i increases the amplitude of absorption peak at f_r because the initial absorption of the porous layer is larger. Similarly, the larger θ^i is the larger is the amplitude of the absorption peak associated with the trapped mode.

To conclude, the HR resonance induce an increase of the absorption coefficient in the viscous regime which is larger when the input impedance is smaller, when the HR spatial density is larger and when the neck is closer to the porous/air interface. At higher frequencies than the viscous regime, this configuration behaves as a 2D one, and can enable to reach a total absorption peak at the trapped mode

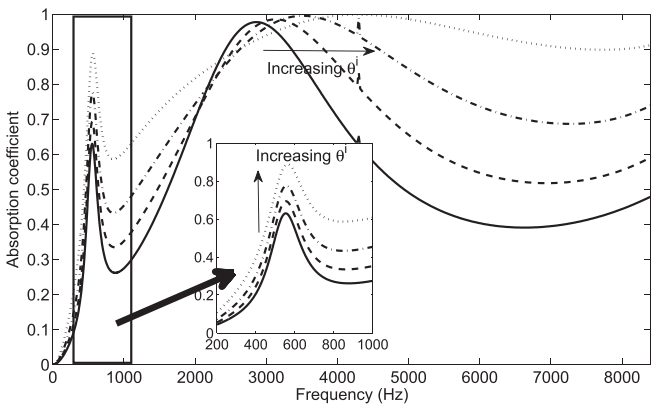

FIG. 4. Absorption coefficient of the configurations $C1$ occupied by the foam $S2$ when excited at $\theta^i = 0$, $\theta^i = \pi/6$, $\theta^i = \pi/4$, and $\theta^i = \pi/3$ for $\psi^i = 0$. The insets show zooms of the absorption coefficient around the HRs frequencies.

resonance frequency for a lower filling fraction than if 3D inclusions would have been embedded in.

B. Results for two HRs per period

It is found to be quite difficult to accurately couple the HRs as it is the case with split-ring resonators,[9,26] particularly when modifying the neck orientation. This can be explained because the opening of a 3D-extruded split ring tends to a slit, which yields a larger coupling surface. A near field coupling of resonators[27] has not been exhibited in our configuration when the HR necks are facing one with each other, even for tiny distance between the necks. The actual coupling between the HRs is also qualified as "far field" coupling. The largest absorption enhancement is obtained when the neck is facing the air interface. The neck x_2-coordinate was also investigated without particular modification of the associated absorption peak.

In what follows, two HRs per period are considered and the coupling between these two HRs is investigated. Either the outer radius or the neck length of one HR is modified in order to widen the large absorption peak associated with the HR resonances. Obviously, the modification of one induce a modification of the other. Figure 5 depicts the absorption coefficient of configuration $C4$ when $l_n^{(2)}$ varies from 4 to 11 mm, and of configuration $C5$ when $r_e^{(2)}$ varies from 8 to 6 mm. Decreasing $l_n^{(2)}$ widen the absorption peak till the HRs are decoupled. The modification of the neck length of one of the HRs does not modify the absorption curve at higher frequencies. Decreasing $r_e^{(2)}$ also widen the large absorption peak till the HRs are decoupled. The absorption follows similar trend when $r_e^{(2)}$ decreases as when $l_n^{(2)}$ decreases. However, the absorption is modified at higher frequencies when $r_e^{(2)}$ is modified. The peak associated with the trapped mode excitation possesses an optimum (in amplitude) for *ff* $= 0.4255$, which means that this filling fraction can be obtained with two different scatterers in case of two scatterers per spatial period. The fundamental modified mode of the backed layer, associated with the periodicity $d_2 = 42$ mm, is excited around 8000 Hz because the unit cell is now quite different from the one containing only one scatterer. This offers the possibility of an absorption enhancement at the location of the Bragg interference by optimizing the excitation of this mode around 6000 Hz.

To conclude, the detuning of HRs in a unit cell enables to widen the enhanced absorption frequency band due the HRs resonance. The modification of neck length is easier and seems to be more efficient than a modification of the volume cavity to achieve this widening.

V. EXPERIMENTAL VALIDATION

The sample is composed of a Melamine foam $S2$ as the porous matrix and two HRs of cylindrical shapes as shown in Fig. 6(a). The brass hollow cylindrical shells are 8 mm outer radius, 6.8 mm inner radius, and 40 mm long. They are closed by two 1 mm thick circular aluminum plates glued on both ends of each shell. Therefore, the total length of the resonator is 42 mm. The x_3 coordinate of both cylinder axis is 11.5 mm, while $x_1^{(1)} = 11.5$ mm and $x_1^{(2)} = 30.5$ mm defining

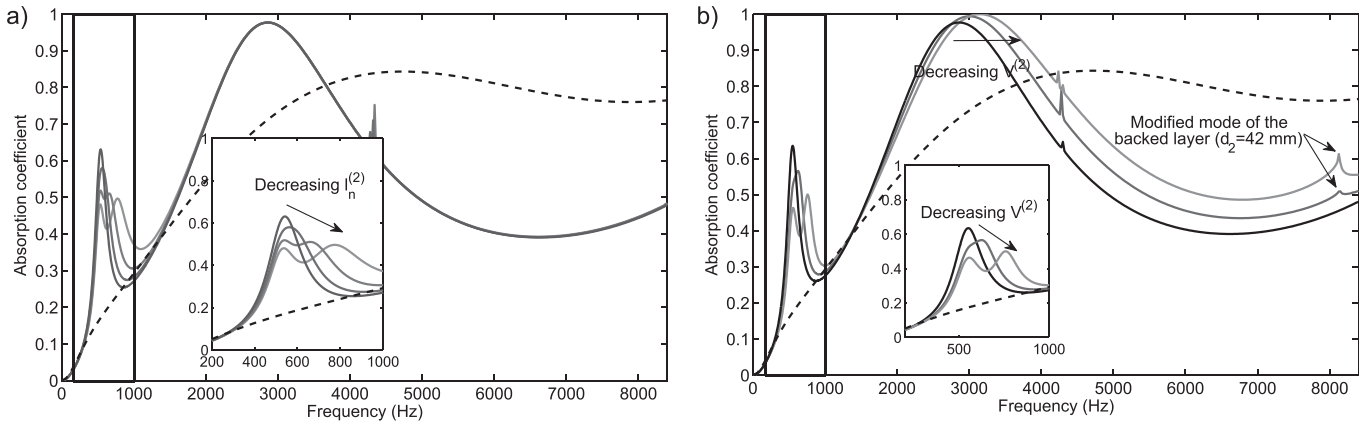

FIG. 5. Absorption coefficient of configurations $C4$ (a) when $l_n^{(2)}$ vary from 4 to 11 mm, and of configurations $C5$ (b) when $r_e^{(2)}$ vary from 8 to 6 mm and of the associated homogeneous sheet (dashed curves) occupied by the foam $S2$ when excited at normal incidence. The insets show zooms of the absorption coefficients around the HRs frequencies.

configuration $C6$. The HRs are drilled at 12 mm from one end with a 4 mm diameter hole. Aluminum necks of inner radius 1.5 mm and length l_n are inserted in. The initial 22.5 mm-thick Melamine foam is drilled and the resonators are embedded in. The sample is placed at the end of an impedance tube having a square cross-section with a side length 42 mm, against a copper plug that closes the tube and acts as a rigid boundary. By assuming that plane waves propagate below the cut-off frequency of the tube 4150 Hz, the infinitely rigid boundary conditions of the tube act like perfect mirrors and create a periodicity pattern in the x_1 and x_2 directions with a periodicity of 42 mm. This technique was previously used in Refs. 9–11 and 20 and allows to determine experimentally the absorption coefficient of a quasi-infinite 3D periodic structure just with one or a correctly arranged small number of unit cells.

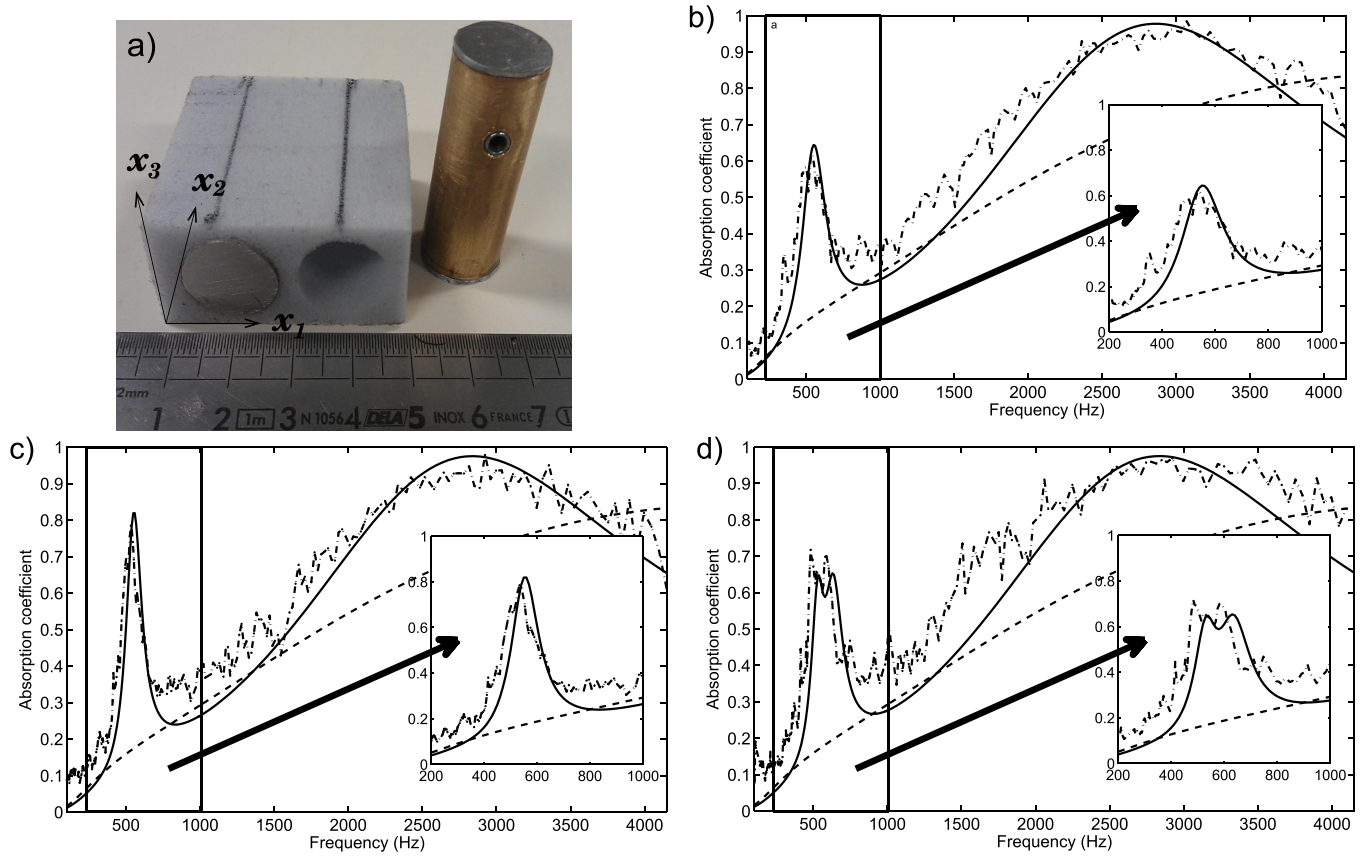

FIG. 6. (Color online) (a) Pictures of the sample. (b) Absorption coefficient of the Melamine foam with two embedded HRs, configuration $C6$. (c) Absorption coefficient of the Melamine foam with two HRs embedded in, configuration $C6$, with a small amount of porous material removed in front of the neck. (d) Absorption coefficient of the Melamine foam with $l_n^{(1)} = 11$ mm and $l_n^{(2)} = 7$ mm HRs embedded in, configuration $C7$, with the porous material removed in front of the neck. FE calculations (solid curves) and corresponding experimental results (dashed-dotted curves) are shown. The insets show zooms of the absorption coefficient around the HRs frequencies. The absorption coefficient of the initial Melamine foam is also shown (dashed line).

The absorption coefficient of this sample is depicted in Fig. 6(b), showing a good agreement between the FE modeling and the measurements. The differences are attributed to imperfections in the sample manufacturing and material parameters. When compared to the initial Melamine plate, the absorption is largely increased around 3000 Hz, because of the excitation of a trapped mode that traps the energy between the cylindrical inclusions and the rigid backing, and around 560 Hz because of the HR resonance. In particular, the absorption coefficient is 0.65 at f_r which corresponds to an increase of nearly 250% of the initial Melamine plate absorption.

When a small amount of porous material is removed just in front of the neck, the input impedance of HRs is smaller allowing the advection to be larger. The amplitude of the absorption coefficient at the resonance frequency of the HRs is 26% larger and reaches 0.82, as shown in Fig. 6(c). The narrowing of the absorption peak is also observed.

The lengths of the HRs necks are modified to be $l_n^{(1)} = 11\,\text{mm}$ ($f_r^{(1)} = 521\,\text{Hz}$) and $l_n^{(2)} = 7\,\text{mm}$ ($f_r^{(2)} = 618\,\text{Hz}$), configuration $C7$, in order to validate the widening of the high absorption frequency band. These two lengths have been determined in order to shift the two modes in frequency to enlarge the enhanced absorption bandwidth but not sufficiently to lead to two separated peaks. While the absorption coefficient is modified around the resonance frequency of the HRs, the absorption coefficient is unchanged at higher frequency [see Fig. 6(d)]. The absorption coefficient is larger than 0.5 over a 120 Hz range (between 500 Hz and 620 Hz) in the case of two identical resonators, while it is over a 190 Hz range (between 500 Hz and 690 Hz) in case of these two different resonators, which represents a widening of 60% of the enhanced absorption bandwidth.

VI. CONCLUSION

The absorption of a small thickness porous foam is enhanced both in the viscous and inertial regimes by periodically embedding HRs. This embedment leads to trapped mode excitation that enhance the absorption coefficient for frequencies lower than the quarter-wavelength frequency and to HR excitation. In particular, a large absorption is reached for wavelength in the air 27 times larger than the sample thickness. The absorption amplitude and bandwidth is then enlarged by removing porous material in front of the HR neck, enabling a lower input impedance of the global effective material, and by adjusting the resonance frequencies of detuned HRs. The numerical parametric analysis and the experimentally tested configurations, pave the way of future development of very thin broadband large absorption metamaterials based on optimized HRs coupled with porous materials. In particular, compound cells with slightly detuned HRs seems to be a promising direction.

ACKNOWLEDGMENTS

This work was partly supported by the ANR Project METAUDIBLE No. ANR-13-BS09-0003 co-founded by ANR and FRAE.

[1]Y. Champoux and J.-F. Allard, "Dynamic tortuosity and bulk modulus in air-saturated porous media," J. Appl. Phys. **70**, 1975–1979 (1991).
[2]X. Olny and C. Boutin, "Acoustic wave propagation in double porosity media," J. Acoust. Soc. Am. **114**, 73–84 (2003).
[3]J.-L. Auriault and C. Boutin, "Deformable porous media with double porosity. III Acoustics," Transp. Porous Media **14**, 143–162 (1994).
[4]O. Dazel, F.-X. Bécot, and L. Jaouen, "Biot effects for sound absorbing double porosity materials," Acta Acust. Acust. **98**, 567–576 (2012).
[5]R. Venegas and O. Umnova, "Acoustical properties of double porosity granular materials," J. Acoust. Soc. Am. **130**, 2765–2776 (2011).
[6]T. Dupont, P. Leclaire, O. Sicot, X. Gong, and R. Panneton, "Acoustic properties of air-saturated porous materials containing dead-end porosity," J. Appl. Phys. **110**, 094903 (2011).
[7]J.-P. Groby, A. Duclos, O. Dazel, L. Boeckx, and L. Kelders, "Enhancing the absorption coefficient of a backed rigid frame porous layer by embedding circular periodic inclusions," J. Acoust. Soc. Am. **130**, 3771–3780 (2011).
[8]B. Nennig, Y. Renoux, J.-P. Groby, and Y. Aurégan, "A mode matching approach for modeling two dimensional porous grating with infinitely rigid or soft inclusions," J. Acoust. Soc. Am. **131**, 3841–3852 (2012).
[9]C. Lagarrigue, J.-P. Groby, V. Tournat, O. Dazel, and O. Umnova, "Absorption of sound by porous layers with embedded periodic array of resonant inclusions," J. Acoust. Soc. Am. **134**, 4670–4680 (2013).
[10]J.-P. Groby, W. Lauriks, and T. Vigran, "Total absorption peak by use of a rigid frame porous layer backed with a rigid multi-irregularities grating," J. Acoust. Soc. Am. **127**, 2865–2874 (2010).
[11]J.-P. Groby, B. Brouard, O. Dazel, B. Nennig, and L. Kelders, "Enhancing the absorption of a rigid frame porous layer by use of a rigid backing with three-dimensional periodic multi-irregularities," J. Acoust. Soc. Am. **133**, 821–831 (2013).
[12]Z. Yang, J. Mei, M. Yang, N. Chan, and P. Sheng, "Membrane-type acoustic metamaterial with negative dynamic mass," Phys. Rev. Lett. **101**, 204301 (2008).
[13]J. Mei, G. Ma, M. Yang, Z. Yang, W. Wen, and P. Sheng, "Dark acoustic metamaterials as super absorbers for low-frequency sound," Nature Commun. **3**, 756 (2012).
[14]S. Kim, Y.-H. Kim, and J.-H. Jang, "A theoretical model to predict the low-frequency sound absorption of a Helmholtz resonator array," J. Acoust. Soc. Am. **119**, 1933–1936 (2006).
[15]S.-H. Seo, "Silencer design by using array resonators for low-frequency band noise reduction," J. Acoust. Soc. Am. **118**, 2332–2338 (2005).
[16]W. Yunker, C. Stevens, G. Flowers, and R. Dean, "Sound attenuation using microelectromechanical systems fabricated acoustic metamaterials," J. Appl. Phys. **113**, 024906 (2013).
[17]C.-L. Ding and X.-P. Zhao, "Multi-band and broadband acoustic metamaterial with resonant structures," J. Phys. D: Appl. Phys. **44**, 215402 (2011).
[18]H. Zeng, C. Luo, H. Chen, S. Zhia, and X. Zhao, "Flute-model acoustic metamaterials with simultaneously negative bulk modulus and mass density," arXiv:1210.2527 (2012).
[19]C. Boutin, "Acoustics of porous media with inner resonators," J. Acoust. Soc. Am. **134**, 4717–4729 (2013).
[20]J.-P. Groby, B. Nennig, C. Lagarrigue, B. Brouard, O. Dazel, and V. Tournat, "Using simple shape three-dimensional rigid inclusions to enhance porous layer absorption," J. Acoust. Soc. Am. **136**, 1139–1148 (2014).
[21]A. Selamet and I. Lee, "Helmholtz resonators with extended neck," J. Acoust. Soc. Am. **113**, 1975–1985 (2003).
[22]D. Johnson, J. Koplik, and R. Dashen, "Theory of dynamic permeability and tortuosity in fluid-saturated porous media," J. Fluid Mech. **176**, 379–402 (1987).
[23]J.-P. Groby, E. Ogam, L. De Ryck, N. Sebaa, and W. Lauriks, "Analytical method for ultrasonic characterization of homogeneous rigid porous materials from transmitted and reflected coefficients," J. Acoust. Soc. Am. **127**, 764–772 (2010).
[24]J.-F. Allard and N. Atalla, *Propagation of Sound in Porous Media: Modelling Sound Absorbing Materials* (John Wiley & Sons, Chichester, UK, 2009), Chap. 5, pp. 73–107.
[25]U. Ingard, "On the theory and design of acoustic resonators," J. Acoust. Soc. Am. **25**, 1037–1061 (1953).
[26]Y. Cheng and X. Liu, "Coupled resonant modes in twisted acoustic metamaterials," Appl. Phys. A **109**, 805–811 (2012).
[27]T. Johansson and M. Kleiner, "Theory and experiments on the coupling of two Helmholtz resonators," J. Acoust. Soc. Am. **110**, 1315–1328 (2001).